Available online at www.sciencedirect.com

SCIENCE DIRECT

Cement and Concrete Research 35 (2005) 233–242

CEMENT AND CONCRETE RESEARCH

Local porosity analysis of pore structure in cement paste

Jing Hu*, Piet Stroeven

Faculty of Civil Engineering and Geosciences, Delft University of Technology, Stevinweg 1, 2628 CN Delft, The Netherlands

Received 26 August 2003; accepted 8 June 2004

Abstract

Three-dimensional (3-D) local porosity theory (LPT) was originally proposed by Hilfer and recently used for the analysis of pore space geometry in model sandstone. LPT pursues to define the probability density functions of porosity and porosity connectivity. In doing so, heterogeneity differences in various sandstone samples were assessed. However, fundamental issues as to the stochastic concept of geometric heterogeneity are ignored in Hilfer's LPT theory. This paper focuses on proper sampling procedures that should be based on stochastic approaches to multistage sampling and geometric heterogeneity. Standard LPT analysis provides a 3-D microscopic modeling approach to materials. Traditional experimental techniques yield two-dimensional (2-D) section images, however. Therefore, this paper replaces the method for assessing material data in standard LPT theory to a more practical one, based on stereological, 3-D interpretation of quantitative image analysis data. The developed methodology is used to characterize the pore structure in hardened cement paste with various water/cement ratios (w/c) at different hydration stages.

Keywords: Cement paste; Heterogeneity; Image analysis; Local porosity theory

1. Introduction

Conventional geometric characterizations of pore structure in experimental as well as in simulation studies particularly focus on porosity, specific pore surface area, pore size distribution, and sometimes on correlation functions. An extensive literature is available on such approaches. Because a different strategy is followed in this paper, no representative referencing is pursued on such approaches, however. Moreover, Scheidegger [1] has pointed out that pore size distribution is mathematically ill defined. Therefore, instead of considering different 'sizes' of pores as the prime source of randomness in porous media, local porosity theory (LPT) [2] proposes considering porosity itself as the random variable. LPT encompasses two geometric characteristics, i.e., local porosity distribution and local percolation probability. In doing so, the fluctuations in porosity as well as in connectivity are recorded. This theory has been used by Biswal et al. [3] to assess heterogeneity of porosity in model sand stones. Unfortunately, some fundamentals of the statistical concept of heterogeneity are ignored in their research. It is the prime purpose of this paper, therefore, to upgrade this approach, correcting for such deficiencies, and to modify the method so that experimental data are more easily obtained.

Heterogeneity is not an intrinsic material property, but a stochastic modeling concept [4–6]. The average values of an arbitrary three-dimensional (3-D) geometric parameter of concrete will be quite alike when obtained from large volumes of the material. Thus, such volumes are defined as homogeneous for the very parameter. The differences between the average values will increase at declining size of the sample volumes. The amount of scatter involved is expressed in standard deviation or coefficient of variation. Alternatively, Lu and Torquato divide the standard deviation by the engineering value of volume fraction and define this as *coarseness*. The coarseness in their study, for arbitrary D-dimensional two-phase anisotropic media and observation region, is shown related to an integral involving the two-point probability function [6]. The sample volume for which the standard deviation in the global values of the selected geometrical parameter is still at an acceptable level is referred to as the representative volume element (RVE) for that particular parameter; this RVE is said to be *homogeneous* as to the same parameter. The same reasoning is followed when sections of similar size of the material are

* Corresponding author. Tel.: +31-15-278-2307; fax: +31-15-278-8162.
E-mail address: J.Hu@citg.tudelft.nl (J. Hu).

0008-8846/$ – see front matter © 2004 Elsevier Ltd. All rights reserved.
doi:10.1016/j.cemconres.2004.06.018

used for the assessment of two-dimensional (2-D) information on a certain geometric parameter. In this case, one of the equally sized area elements yielding an acceptable scatter level in the geometric data is defined as homogeneous for the associated 2-D geometric parameter, and denoted by representative area element (RAE). Thus, the degree of heterogeneity depends for a given sample size on the type of geometric parameter, and on the sample size for a specific geometric parameter [4,5]. A sample of (at least) the size of the RVE/RAE would be necessary when unbiased estimation of bulk features is pursued; then, the material is considered on macroscopic or engineering level. Because properties and structural features are directly related, the aforementioned reasoning and terminology can also be extended to cover material properties. The LPT approach is dealing with local porosity, and with scatter among measuring data on a submacroscopic (i.e., sub-RVE) level. Pores are smeared out for that purpose in a *sufficiently large volume element* between a microscopic level where single pores are visualized and the macroscopic one.

A logic consequence of the sketched stochastic heterogeneity concept is that comparison of different populations demands operating with similar probing sensitivity. Hence, the size ratio of sample and RVE/RAE should be constant. Only under such conditions are the heterogeneity influences normalized and separated from the mean estimates. Unfortunately, these fundamental requirements are rarely fulfilled by engineers in the field of material science, an example being the LPT study by Biswal et al. [3]. Moreover, direct characterization by LPT is only possible on the basis of a *reliable* 3-D structure model of porous media. For actual cement pastes, such models cannot be derived from the available 2-D section images. Hence, 3-D LPT is not directly applicable to scanning electronic microscopy (SEM) images. In this study, 2-D local porosity analysis is therefore proposed as an analogue of 3-D LPT. It simplifies computation and maintains the characteristics of the pore structure directly obtained from cement paste. In this paper, the porosity distribution and percolation probability in cement pastes with various water/cement ratios (w/c) at different degrees of hydration are studied with 2-D LPT. This information is acquired by quantitative image analysis of polished sections of the actual cement paste. Stereology allows for 3-D interpretation of such data.

2. Fundamentals and definitions

When the researcher is trying to assess the influence(s) of a certain regime on the material of interest in the engineering construction, the material is molded or shaped (e.g., by sawing) so it can be subjected in a convenient way to the regime at issue. In stochastic terms, the material in the construction constitutes the *population*, while a certain number of 'identical' specimens can be seen as the *sample*. Specimens reveal fluctuations due to their restricted dimensions in material structure, and, as a consequence, also in their behavior when subjected to the external regime. This is denoted as *between-specimens* scatter. A major part of the engineering research has this *first sampling stage* as terminus. As an example, the average compressive strength of a series of specimens is seen in such research efforts as an unbiased estimate of the material strength in the construction, whereby reliability is associated with the aforementioned scatter. When so-called size effects (basically, heterogeneity effects) are recognized, the estimates can be corrected to serve the engineering purpose.

However, with structural research, we have to add *additional sampling stages*. The specimens are cut to yield *sections*, of which location and orientation should be randomized, unless the researcher has strong arguments that allow release of this requirement. Sections, and associated images that can be visualized (mostly, by artificial means) at the section surface, have dimensions smaller than those of the specimen (at least to avoid disturbed boundary layers). These section images represent a set of different locations and orientations of a specimen body previously subjected to the regime. Similarly located and oriented section images of repeated experiments reveal *between-sections* scatter at the so-called *second sampling stage*. Of course, this equally holds for the result of the averaging operation over a set of sections randomized with respect to location and orientation.

Section images are too large in general to be subjected to quantitative microscopy. Instead, fields significantly smaller than the section area are employed for that purpose. This is the *third sampling stage*, confronting the researcher with *between-fields* scatter, which depends, of course, on the size of the fields. The fields are finally submitted to stereological methods of quantitative image analysis. The procedure might be repeated randomly a number of times, revealing variation among the data. Fortunately, this in-field scatter can be estimated for an optimized image analysis design. This is, however, not of prime relevance here. Nevertheless, it can be imagined that scatter will be directly governed by extent of the geometrical parameter in the field and the grid line density. It is the fourth and last contribution in this *four-stage sampling strategy* to overall scatter.

The optical magnification required for visualization of the material microstructure at the level of the researcher's interest defines both the microstructural level displayed by the field, and the geometric structure of the RVE. Hence, *optical resolution* and observed *level of the microstructure* are intimately connected: higher densities of geometric parameters will be observed under higher optical resolution. This has nothing to do with material properties, but is a direct reflection of the research strategy.

The *reliability of the engineering estimate* for material behavior (in terms of the observed geometric material parameters) under the external regime depends, of course, on the overall scatter, i.e., reflecting the four-stage sampling

process involved in the research efforts. Only the between-fields scatter is referred to in many published approaches, which nevertheless derive their relevance from application of the results to engineering problems. This should also be kept in mind when focusing in the present paper on only the last stage in this sampling design.

The following terminology for a proper sampling strategy—in agreement with the foregoing—is adapted for this paper.

- Unbiased estimation should be based on so-called RVEs. Alternatively, when working with section images, as in the present case, RAEs should be involved. They are both defined as elements of which the linear dimensions are sufficiently large to guarantee *heterogeneity in the geometric parameter of interest to be reduced to an acceptable level*. Thus, the RVE and RAE are by definition homogeneous as to the geometric parameter at issue.
- The RAE is divided in subareas on a certain level of the microstructure. Fields are selected by a randomized (or systematic) procedure among these subareas. Probing level should be similar for cases of a comparative study, involving a *constant size ratio of fields and RAEs*. This is denoted as the probing sensitivity. For example, in a study of differently matured cement pastes, the RVEs will have different dimensions. Fulfilling the requirement of constant probing sensitivity will involve using fields of different sizes.
- The optical resolution defines minimum dimensions of the microstructure (in the present case, of pore diameters) of the RVE/RAE that can be studied in the field image. Hence, it also governs the level of the microstructure, which is revealed by the RVE/RAE. For comparative studies, the level of the microstructure should be similar, involving a *constant size ratio of minimum and RVE/RAE dimensions*. For example, a study of the evolving pore structure in cement paste should be based on different sizes of RVEs, different sizes of fields (equal probing sensitivity), and different optical resolution levels (but equal size ratio of smallest pores and RVE).

This paper focuses on the very last stage in the aforementioned four-stage sampling process. Because the information on pore characteristics obtained in this way should be representative for the engineering level, where we are confronted with durability aspects of civil engineering structures in which the material is employed, extreme care should be bestowed on a careful design of the experiments involving all four sampling stages. It is noteworthy to remark that a more closer study of the various contributions to overall scatter (and, thus, to reliability of the estimates) will inevitably lead to the Golden Rule earlier formulated by Gundersen [7]: 'Do more less well'. This implies that, in many cases, an increase in the number of specimens is far more efficient in increasing reliability than selecting an excessive number of fields, and, even more, in intensifying the image analysis operation. The latter, however, is the general trend because of automation possibilities. Still, it will be the weakest link in such a chain that is disproportionately affecting the reliability of engineering estimates. An optimized approach requires paying explicit attention to a design leading to equal contributions to scatter at the different sampling stages. Last, but far from least, the aforementioned fundamental requirements should be fulfilled. This aspect receives particular attention in this paper, showing the major consequences of violating such requirements.

3. Theoretical background

3.1. Statistical concept of heterogeneity

Engineering properties are supposed to reflect certain aspects of the behavior of material elements of at least representative dimensions. In such RVE, the material parameter at issue can be smeared out at a specified probability level. Each geometrical parameter has its independent scale of homogeneity with corresponding size of RVE [4]. Heterogeneity of the selected parameter will increase inside the RVE/RAE with a decline of the microstructural level taken into consideration and defined by the selected resolution of observations (e.g., SEM) or measurement equipment (e.g., strain gauges).

In summary, heterogeneity is a function of the selected material parameter and of probing sensitivity, i.e., the ratio of linear dimensions of the field or probe to that of the RVE/RAE involved [5]. Insight into the size of the RVE is therefore crucial for the sampling strategy, and thus for the economy of the experiment. When dealing with different populations, it is also a prerequisite for unbiased comparison of outcomes.

3.2. 3-D LPT

LPT measures porosity and other geometric observables within a bounded (compact) volume of the porous medium. These measurements are collected into various histograms (empirical probability density) by means of δ function (delta function) [8]. It is a generalized function defined as the limit of a class of delta sequences. In engineering contexts, the functional nature of the delta function is often suppressed, and δ is instead viewed as a special kind of function, resulting in the useful notation [8]. The type of δ function used in this study will be described in Section 3.3.

The sample set S contains two disjoint subsets, pore space P and solid matrix M (composed of unhydrated cement and hydration products). Let $K(x,L)$ denote a cube of side length L centered at the lattice vector x in discretized model sample. The set $K(x,L)$ defines a measurement cell inside which local geometric properties, such as porosity,

can be measured. The local porosity in this measurement cell is denoted as $\phi(x,L)$.

The local porosity distribution $\mu(\phi,L)$ is defined as

$$\mu(\phi,L)=\frac{1}{m}\sum_{x}\delta(\phi-\phi(x,L))$$

with δ function:

$$\delta(\phi-\phi(x,L))=0 \text{ for } \phi\neq\phi(x,L) \quad (1)$$

where m is the number of placements of the measurement cell.

The function $\mu(\phi,L)$ measures the probability to find the local porosity ϕ in the range from ϕ to $\phi+\mathrm{d}\phi$ in a cell of linear dimension L.

The second geometric property to characterize local geometry indicates whether pore space percolates or not. A cell $K(x,L)$ is called 'percolating in the x direction' if there exists a path inside the pore space connecting those two faces of the measurement cell that are perpendicular to the x axis. The definition is similar for other directions.

Let

$$\Lambda_{\alpha}(x,L)=\begin{cases}1 \text{ if } K(x,L) \text{ percolates in } \alpha \text{ direction}\\ 0 \text{ otherwise}\end{cases} \quad (2)$$

be an indicator for percolation. The definition of 'α' direction is given in Table 1. Thus, $\Lambda_3=1$ indicates that the cell can be traversed along all three directions, while $\Lambda_1=1$ indicates that there exists at least one direction along which the cell is percolating. $\Lambda_0=1$ indicates a blocking cell.

The local percolation probability in the 'α' direction is now defined through

$$\lambda_{\alpha}(\phi,L)=\frac{\sum_x \Lambda_{\alpha}(x,L)\cdot\delta(\phi-\phi(x,L))}{\sum_x \delta(\phi-\phi(x,L))} \quad (3)$$

Thus, $\lambda_{\alpha}(\phi,L)$ denotes the fraction of cells (with side length L and local porosity ϕ) percolating in the 'α' direction. Pore space in cement paste is fully connected at $\lambda_3=1$. It is an important geometric quantity for physical properties of porous media, such as permeability. The calculation of $\mu(\phi,L)$ and $\lambda_{\alpha}(\phi,L)$ is fairly straightforward. For details, see Refs. [2,3].

Table 1
Definition of 'α' direction

Index α	Meaning
x	x direction
y	y direction
z	z direction
3	$(x\wedge y\wedge z)$ direction
1	$(x\vee y\vee z)$ direction
0	$(\neg(x\vee y\vee z))$ direction

3.3. Conversion to 2-D LPT

Observations should provide 3-D information on structure of materials. Opaque materials, like the cementitious ones, do not allow easy access to 3-D material structure, however. Geometrical statistical (i.e., stereological) tools should therefore be applied for this purpose, because they provide means for unbiased estimation of 3-D geometrical parameters of the state of aggregation on the basis of one-dimensional or 2-D observations [5].

The area fraction of pore space A_A in a measurement square is an unbiased estimator of the volume fraction of pores V_V, i.e., porosity in a measurement cell [9]. The local porosity in a measurement square (field) of side length L on section image can be easily determined. The local porosity distribution curve of $\mu(\phi,L)$ can be obtained in a similar way as in the 3-D case. The δ function can take different forms. In this study, the following δ function is used:

$$\delta(t)=\frac{\zeta}{\pi(\zeta^2+t^2)} \qquad \text{with}\,\zeta=0.001 \quad (4)$$

The δ function plotted against t appears like a very tall and narrow spike (at $t=0$) of height $1/\pi\zeta$ and width of about $\pi\zeta$. The δ curve vanishes outside a very narrow range symmetric around $t=0$. This operation conveniently collects measuring data of local porosity into a histogram and yields a continuous curve of porosity density distribution.

The local percolation probability in a measurement square makes little sense because the percolation probability of porosity is much lower in 2-D section than in three dimensions. Scher and Zallen [10] proposed 'universal' values for the percolation threshold at 45% in two dimensions, and 16% in three dimensions. This means that the 3-D porosity is still highly connected at a total porosity of 45% while appearing to be blocked in 2-D porosity. Scher and Zallen's results also qualitatively confirm the general observation that, in cements, the pore space appears discontinuous in 2-D micrographs far earlier than it actually becomes discontinuous in three dimensions. Bentz and Garboczi [11] proposed an approximately 18% porosity as the depercolation threshold; this means that the porosity network will depercolate when the porosity falls below 18%. This statement is in reasonable agreement with the 'universal' value of Scher and Zallen. Recent publications of Bentz and Garboczi revealed that the depercolation threshold of capillary porosity in ordinary cement is also dependent on cement fineness [12,13]; that is, coarser cement has a lower depercolation threshold of porosity than finer cement. The depercolation threshold of porosity is around 18–21% for cement paste with *ordinary fineness*. Garboczi and Bentz [14] stated that knowledge of the 3-D percolation threshold can be utilized by researchers working on 2-D micrographs of a hydrated cement paste. For example, if the capillary porosity quantified by image

analysis is 25%, it is likely that the capillary porosity is still connected in three dimensions. In this study, the indicator for percolation of a measurement cell is determined in view of the local porosity instead of considering whether there exists a connecting path in the pore space. This approach simplifies the computation required for the determination of percolating or blocking for a measurement cell as accomplished in the 3-D LPT analysis. Because the local porosity in a measurement square can be easily determined, the indicator for 3-D percolation can be defined as follows:

$$\Lambda_3(x,L)=\begin{cases}1 & \text{if } 0.45\le\phi\\ 1.8(\phi-0.18)^2 & \text{if } 0.18<\phi<0.45\\ 0 & \text{if } \phi\le 0.18\end{cases} \quad (5)$$

where $1.8(\phi-0.18)^2$ is the 3-D connectivity of porosity proposed by Garboczi and Bentz [14]. It should be noted that this equation is valid for cement with moderate value of specific surface area (300–400 m^2/kg). If the cement fineness is at a relatively low level (say, 150 m^2/kg), the threshold value will decrease to about 7–8%. When the percolation indicator is determined by Eq. (5), the local percolation probability λ_3 can be calculated according to Eq. (3).

Directional measurements by the authors based on the covariance function (covariance measurements reflect the anisotropy of the structure, see Ref. [15] for details) of model cement pastes suggested that ordinary cement paste can be considered as an isotropic structure on a sufficiently high level of the microstructure. For a presumably isotropic structure, like ordinary cement paste, the percolation probability should be identical in x, y and z directions. In this case, the following relations should hold for the percolation probability. Of course, Eq. (6) basically only hold for RVE/RAE-sized samples, because percolation probability is sensitive to configuration. Hence, all λ values of smaller units will yield biased estimates of engineering values. This relatively small effect (with respect to possible depercolation threshold values) is neglected in this paper.

$$\begin{aligned}\lambda_x&=\lambda_y=\lambda_z\\ \lambda_3&=\lambda_x^3\\ \lambda_0&=(1-\lambda_x)^3\\ \lambda_1&=1-\lambda_0=1-(1-\lambda_x)^3\end{aligned} \quad (6)$$

Hence, local percolation functions in particular directions can be derived from λ_3.

4. Materials and methods

4.1. Sample preparation and image analysis

The sample preparation and the image acquisition procedures pertaining to cement paste specimens are described in Ref. [16]. Two w/c are involved in this study, 0.4 and 0.6, respectively. The absolute size of each image is 263 μm in length and 186 μm in width (1424 × 968 pixels). The optical resolution of SEM image is 0.18 μm/pixel. The SEM image was made of a polished section of cement paste and transformed into a binary image with pores as phase of interest. A measurement square (field) of side length L was systematically placed in all possible locations within the image frame. For the placement strategy of the fields, see Ref. [3]. Local porosities were measured over a wide range of field sizes L from 9 to 66 μm.

4.2. Representative area element

In an isotropic material, the representative element can be imagined as a cube in 3-D space or a square in two dimensions. A simple statistical test can be employed to estimate the linear dimension L_{RAE} of the RAE [17]. At a certain value of L, a series of local porosity data are recorded with average value of $\bar{x}$ and standard deviation σ. The coefficient of variation ε is defined as the ratio of σ and $\bar{x}$. The number of observations N can be calculated which is necessary to guarantee that the average value will be within an interval with acceptable range of deviation Δ at a given confidence level (90% in this study). Because it is equivalent to take N samples with area L^2 or to take a single sample with an area of NL^2, the linear dimension of RAE can be estimated to be $\sqrt{N}L$. Taking $\Delta=0.1\bar{x}$, L_{RAE} is calculated for cement pastes with various w/c at different degrees of hydration (Table 2). The linear dimension of RAE is averaged over the results obtained from different values of L (19, 38 and 66 μm, respectively). Once an RAE has been determined for a certain case (porosity in this study), its statistical heterogeneity can be explored.

Table 2 shows that the available images in this study are in two out of the three cases smaller than the RAE. This is due to the necessary resolution to detect pores with an area

Table 2
Comparison between cement pastes (w/c = 0.6) at a similar level of microstructure

Hydration age (days)	3	7	14
L_{RAE} (μm)	202	267	441
L^* (μm)	33	40	66
Porosity $\bar{x}$ (%)	43.15	33.52	24.21
Porosity range (%)	8~73	9~53	10~37
Standard deviation σ (%)	9.75	7.46	5.42
Coefficient of variation ε (%)	22.6	22.3	22.4
χ^2_{exp} [16 classes, $\chi^2(0.1,15)=22.307$]	14.73	10.86	11.55
χ^2_{exp} [20 classes, $\chi^2(0.1,19)=27.204$]	18.59	13.02	21.12

smaller than 0.1 μm^2. Material properties are denoted as *structure insensitive* when solely governed by geometric parameter 'material composition' (volumetric average), e.g., mass or Young's modulus. Contrary, *structure-sensitive* properties, such as the crack initiation strength, are affected by the so-called 'group pattern or configuration of particles' [4,5,18]. The linear dimension of the RVE for structure-sensitive properties will exceed those for structure-insensitive ones to a considerable degree [4,5]. The current image size is selected to compromise between an acceptable representativeness of the section image and a satisfactory image resolution. On the other hand, comparison of heterogeneity in porosity between cement pastes can be made as long as it is based on the same level of microstructure of different specimens (i.e., the same probing sensitivity), regardless of specific RAE size.

4.3. Level of microstructure

One of the purposes of this study is to compare the heterogeneity of porosity in cement pastes at different hydration ages (3, 7 and 14 days, respectively). Hydration will gradually transfer cement paste into a matured material with lower porosity. During the hydration process, the size of the RAE will gradually increase due to a declining number of pore *features* per unit of volume/area. When the structure of cement paste is modified by hydration, a similar level of the microstructure (same probing sensitivity) should be adapted for comparison purposes in experimental designs pursuing a study of the effects of such changes on porosity. Unless this is properly arranged, artificial effects will be mixed with fundamental ones [5]. This obligatory requirement can be fulfilled by taking the ratio L/L_{RAE} constant for cement pastes at different hydration ages.

5. Results and discussion

5.1. Influence of L on local porosity distribution

Fig. 1 shows the local porosity distribution $\mu(\phi,L)$ for paste (w/c = 0.6) at 14 days hydration with field sizes L of 9, 38, 47 and 66 μm, respectively, with the L_{RAE} of 441 μm (see Table 2). The curve resembles to a closer extent the normal distribution as field size gradually increases to L_{RAE}. The μ curves exhibit the typical transfer stages between the limits $L = 0$ and $L \to \infty$. The shape of μ curve depends strongly on L, revealing two competing effects [2,3]. At small L, the local geometries are simple in the rather small field, but the between-fields correlations are strong. At L equal to the sample size, μ does not contain complex geometrical correlations because there is only one measurement cell. At large L, the local geometries are statistically uncorrelated but each one of them is nearly as complex as the whole pore space. There exists an intermediate length scale at which, on one hand, the local geometries are relatively simple, whereas on the other hand, the single-cell distribution function has sufficient nontrivial geometric contents to be a good approximation of the investigated structure.

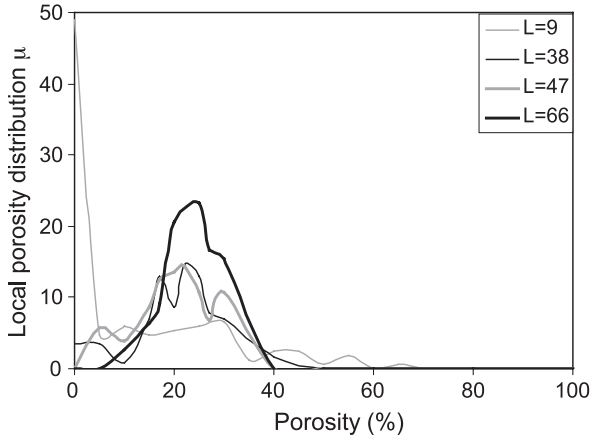

Fig. 1. Local porosity distribution $\mu(\phi,L)$ for cement paste with w/c = 0.6 at 14 days hydration, at linear probe sizes L of 9, 38, 47 and 66 μm, respectively.

The μ curves in Fig. 1 manifest the changes imposed by the two competing influences at increasing L. For L significantly exceeding L_{RAE}, the μ curve should have a unique peak at the value of global porosity and a width approximating zero. This indicates that the paste approaches macroscopic homogeneity at $L \to L_{RAE}$. Because of stochastic influences, the curve will have increasing width at declining L (as shown in Fig. 1), but average porosity pertaining to μ curve will yield global porosity to be the same because of its composition character. To put it in a simple way, the closer the observation with probe size exceeding pore spacing, the more heterogeneous will appear the structure. Hence, observations on different levels of the microstructure will produce according to the theory systematically different information on the degree of heterogeneity, which will be discussed in what follows.

5.2. μ Curves for pastes at different hydration times

The pore microstructure is changing during the hydration process because pore space is gradually filled up with hydration products. As a result, total porosity, critical pore size and mean pore size decrease with hydration time, while the pore size distribution becomes narrower, as earlier demonstrated by the authors by way of image analysis [19]. Fig. 2 presents the local porosity distribution μ of a cement paste (w/c = 0.6) at different hydration times, maintaining the same field size $L = 19$ μm. The differences between a relatively mature paste (at 14 days hydration) and early-age pastes (at 3 and 7 days hydration, respectively) are clear. The shape of the μ curves for pastes at 3 and 7 days hydration are similar, with the curve for the 7-day paste shifting to the left of the 3-day curve. This shifting is due to

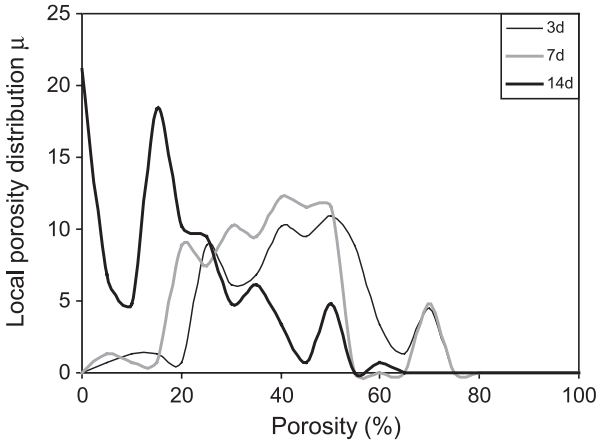

Fig. 2. Local porosity distribution μ for cement paste with w/c = 0.6 at 3, 7 and 14 days of hydration, respectively, at constant linear probe sizes L = 19 μm.

the lower porosity in the 7-day paste. If the field size L is close to L_{RAE}, the porosity distribution curve should resemble the normal distribution. The shape of the μ curve for paste at 14 days hydration (Fig. 2) is far more deviating from the normal distribution than the other two pastes, indicating this paste to have the largest RAE. Correspondingly, heterogeneity of porosity in cement paste is seemingly increasing during the hydration process, when based on probes of similar size.

A general trend in pore structure evolution during hydration is a significant decline in the volume of large pores, whereas the volume of small pores stays relatively constant. The reduction of the volume of large pores is predominant in the early stage of hydration. At first, hydration products are formed in larger pores and later on in the smaller ones, thus leaving initially the volume of small pores more or less constant [20]. This explains the similarity between the 3- and 7-day curves. Once the larger spaces, i.e., voids >0.13 μm, are filled, further hydration would affect the entire pore size distribution. This can account for the obvious difference between the 14-day paste and less mature pastes (at 3 and 7 days hydration).

As a result of further hydration, the pore space gradually changes from a fully connected structure to a depercolated network with some isolated pores. In the viewpoint of statistics, the scatter of porosity distribution is increasing during hydration process due to decline in the number of pore *features* observed in the investigated field of section image. Therefore, for cement paste with 14 days hydration, the scatter of porosity distribution is larger than for less mature paste. When observations are based on fields of similar size, this larger scatter is corresponding to a seemingly more heterogeneous pore structure. This explains the increasing linear dimension of the RAE for porosity homogeneity during hydration.

Studying the heterogeneity of porosity in cement pastes hydrated to different extents requires modifying field sizes to the same proportion of the RVE/RAE. This renders possible properly comparing outcomes on the same level of microstructure unless the sample size is exceeding the linear dimension of RVE/RAE considerably. This type of problem is explicitly discussed in Ref. [5]. When L_{RAE} exceeds image size as in this study, the same 'level of microstructure' (i.e., the same coefficient of variation in the geometric parameter at issue) can be achieved by taking the ratio of L to L_{RAE} constant for all investigated specimens. This specific value of field size is denoted as proportional length scale L^* (Table 2).

Fig. 3 presents the measurements based on the same level of microstructure. The μ curves for three pastes (w/c = 0.6, at 3, 7 and 14 days hydration) are normalized by their respective peak value so that all curves have a maximum value of 1. The curves resemble each other far more closely than in Fig. 2. The peak values of porosity of the three curves can be made to coincide when the aging effect is eliminated. Because the displayed measurements are based on equal scatter of local porosity in the total sample images, theoretically, the three μ curves should be identical and should conform to the normal distribution. The deviations from the normal distribution seem not to be too alarming, seeing also the limited (i.e., subrepresentative) sizes of the sample images. Whether the deviations are significant or not can be checked by applying a χ^2 test. It is a standard statistics tool to evaluate differences between experimental distribution data and corresponding theoretical values. For details of this method, the reader is referred to statistics textbooks, an example being the book by Hoel [21]. This method is also widely used in concrete technology (see, e.g., Ref. [22]).

The local porosity data are collected into traditional histograms in the first step of the χ^2 test. According to the rule of thumb [21], the number of classes n should be roughly the square root of the number of observations. Two values of n are taken into consideration, 16 and 20,

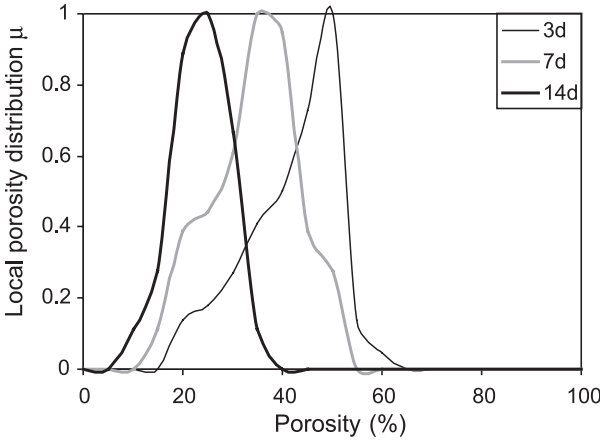

Fig. 3. Local porosity distribution μ measured at the same level of microstructure: L^* = 33, 40 and 66 μm for pastes (w/c = 0.6) at 3, 7 and 14 days of hydration, respectively. The values of μ are normalized by their respective peak values.

respectively. In the case of $n=16$, the class intervals are 4.1%, 2.8% and 1.7%, for 3-, 7- and 14-day pastes, respectively. When $\bar{x}$ and σ are known, the theoretical value of relative frequency of occurrence f_{th} within a class can be calculated according to the normal distribution function. The measured frequency of occurrence is denoted as f_{exp}. The experimental value of χ^2 is calculated as:

$$\chi^2_{exp} = \sum_{i=1}^{n} \left\{ \frac{(f_{exp} - f_{th})^2}{f_{th}} \right\}_i \quad (7)$$

The results are listed in Table 2. In both cases of $n=16$ and $n=20$, the theoretical values of χ^2 exceed those of χ^2_{exp}. Hence, at the 90% probability level, there is no reason to reject the hypothesis that, in all cases, porosities were distributed according to the normal distribution, and as a consequence, Fig. 4 reflects the natural law of the statistical concept of heterogeneity. For L slightly smaller than L^*, local porosity distribution might still be approximated at high probability level by the normal distribution. Thus, the characteristic length scale can be properly assessed as the minimum probe size L_{min} whereby the μ curve can be approximated at a given probability level by the normal distribution function.

These observations are based on images made with the same optical resolution. It should be noted that measurement sensitivity should also be adjusted to the size of the RAE to get an objective situation. Hence, optical resolution of SEM image should have been somewhat reduced during maturation, so that the ratio of minimum pore size detected to L_{RAE} should have been similar for pastes at different hydration ages. This would have made observations on the same level of the microstructure even more pronounced due to the extra reduction in total porosity (governed by image resolution) for more mature paste.

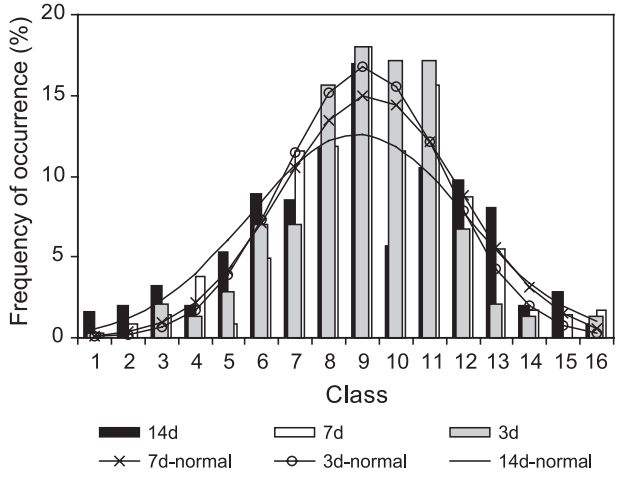

Fig. 4. Conventional histograms of relative frequency of occurrence in porosity distributions for pastes (w/c = 0.6) at 3, 7 and 14 days of hydration, respectively. The experimental values are indicated as columns and the approximated normal distribution curves are shown as continuous lines. χ^2 tests revealed that local porosity distributions conform at 90% probability level to normal distributions.

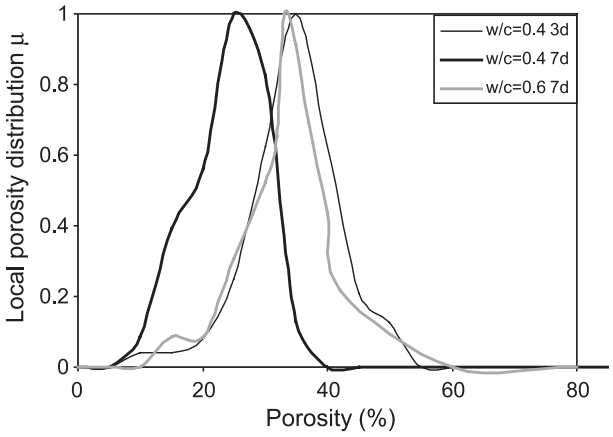

Fig. 5. Local porosity distribution μ for cement paste with w/c of 0.4, at 3 and 7 days hydration, at their characteristic length scales $L_{min}=40$ and 45 μm, respectively; the μ curve for cement paste with w/c of 0.6 at 7 days hydration ($L=45$ μm) is also indicated for comparison purpose. The values of μ are normalized by their respective peak values.

5.3. μ Curves for pastes with different w/c ratios

The local porosity distribution curves for cement pastes with different w/c are shown in Fig. 5 at their respective characteristic length scales. It can be seen that the pore space characteristics of cement paste with w/c = 0.4 at 3 days hydration are almost equivalent to those of paste with w/c = 0.6 at 7 days hydration. The similarity in pore structure between cement paste with relatively low w/c at early age (say, 3 days hydration) and paste with higher w/c at some weeks hydration (1 week or more) is supported by 3-D computer simulation results of Bentz and Garboczi [11]. At the same hydration age, cement paste with w/c = 0.4 is more heterogeneous than the paste with w/c = 0.6 when based on the same probe size. This is reflected by the larger value of L_{min}. This can be partly explained by the influence of w/c on morphology of porosity. The higher the w/c, the more space is available for the undisturbed growth of hydration products. Particularly in the early stage of hydration, when ettringite needles are formed, the available space determines the morphology of the hydration products, which in turn determines the morphology and distribution of porosity. Hence, for a cement paste with higher w/c, the spatial constraints to hydration products are less, and, it is easier for cement paste to reach a relatively homogeneous distribution of porosity via dissolution and precipitation of hydration products.

5.4. Local percolation probability

The local porosity distribution and local percolation probability are shown in Fig. 6 for cement paste with w/c = 0.4 at 3 days hydration, at $L=56$ μm. The μ curve is

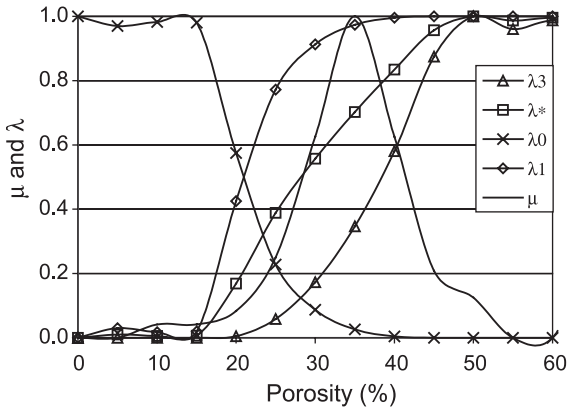

Fig. 6. Local porosity distribution μ and local percolation probabilities λ_α for cement paste with w/c = 0.4 at 3 days hydration, at the characteristic length scale $L = 40$ μm; λ^* represents the local percolation probabilities in x, y and z direction ($\lambda_x = \lambda_y = \lambda_z$).

rescaled so that its maximum equals 1. For this cement paste, the μ curve has its peak value at a porosity of 35%. The λ_3 curve ascends from zero to unity at increasing porosity, but its increase is not always strictly monotonous due to connectivity heterogeneities at intermediate scale levels. The local percolation probabilities are derived according to Eq. (6). The six local percolation functions λ_α provide useful information about pore space. The λ_1 and λ_3 curves constitute lower and upper bounds, respectively, for the region inside which the connectivity increases from 'blocking' to 'fully connected'. If the band between λ_1 and λ_3 curves shifts to the left of the μ curve's peak, then the sample is well connected. The μ curve in Fig. 6 partially overlaps the band from λ_1 to λ_3, which indicates that the permeability of this paste is relatively low.

Fig. 6 reveals obvious changes in pore connectivity to occur over the 20–40% porosity range. This is in agreement with experimental results obtained by Parrott et al. [23] and by Powers [24]. Parrott et al. [23] measured diffusion parameters at various ages for ordinary cement paste and found a large drop in diffusion coefficients when porosity decreased from 40% to 20%. Powers [24] observed a sharp increase in permeability of various cement pastes as capillary porosity increased from 20% to 40%.

The μ curve for mature paste shifts to the left of the λ_1 to λ_3 band. For pastes with higher w/c, the change from blocking to percolating occurs in the low porosity tail of μ, indicating a high degree of connectivity.

It should be noted that the depercolation threshold of porosity is structure sensitive. In a morphological approach, Hu and Stroeven [25] revealed that the particle size distribution of model cement has significant influences on the depercolation threshold of porosity, whereas the effect of w/c on this threshold is minor. The depercolation threshold of porosity is around 18–21% for cement paste with *ordinary fineness*. W/c is a *composition* parameter because it represents the mass/volume fraction of cement in the material mixture. Contrary, when particle size distribution is varied, spacing parameters, including interparticle spacing and nearest neighbor distances, are involved, which constitute a *configuration* issue [5,22].

6. Conclusions

This paper deals with porosity distribution fluctuations in cement pastes with various w/c at different degrees of hydration. Some fundamentals are emphasized about the statistical concept of heterogeneity that are frequently ignored in studies of materials. At a given w/c, the linear dimensions of the RAE for porosity homogeneity increase with hydration time. The size of the RAE is larger for cement paste with lower w/c, corresponding to a more heterogeneous structure considered on fields of similar size. When the comparison between various cement pastes is based on the same level of microstructure, however, the local porosity distribution curves can be approximated by normal distribution functions. These normal distribution curves are similar for various cement pastes, provided normalized by peak frequencies and after elimination of age effects. This confirms that heterogeneity is not a material characteristic, but a function of the geometric material parameter at issue, of the microstructural level taken into consideration and of the linear dimension of the RAE involved.

As an alternative to the 3-D LPT proposed by Hilfer, a 2-D LPT is developed in this study, and is combined with quantitative image analysis of specimen sections to characterize the 3-D porosity distribution and percolation probability in cement paste with various w/c at different degrees of hydration. The conversion from three dimensions to two dimensions is based on two points: (1) area fraction of porosity is an unbiased estimate of volume fraction of porosity; (2) knowledge of porosity at the percolation threshold and quantitative empirical relationship between connectivity and porosity.

Local porosity distribution and percolation probability curves are valuable sources of information for estimating permeability or diffusion quality of cement paste. This allows a logic approach to assessing durability capacity of concrete.

References

[1] A.E. Scheidegger, The Physics of Flow through Porous Media, University of Toronto Press, Toronto, 1974.
[2] R. Hilfer, Geometric and dielectric characterization of porous media, Phys. Rev. B 44 (1991) 60–75.
[3] B. Biswal, C. Manwart, R. Hilfer, Three-dimensional local porosity analysis of porous media, Physica A 255 (1998) 221–241.
[4] A.M. Freudenthal, The Inelastic Behavior of Engineering Materials and Structures, Wiley, New York, 1950.
[5] P. Stroeven, Implications of the law of aggregation of matter in concrete technology, in: A.M. Brandt, V.C. Li, I.H. Marshall (Eds.), Proceedings of BMC7 (Brittle Matrix Composite), Poland, 2003, pp. 129–142.

[6] B. Lu, S. Torquato, Local volume fractions in heterogeneous media, J. Chem. Phys. 93 (1990) 3452–3459.
[7] H.J.G. Gundersen, R. Osterby, Optimizing sampling efficiency of stereological studies in biology: or "Do more less well", J. Micros. 121 (1981) 65–73.
[8] R. Bracewell, The impulse symbol, (Chapter 5). The Fourier Transform and Its Applications, 3rd edition, McGraw-Hill, New York, 1999, pp. 69–97.
[9] E.E. Underwood, Quantitative Stereology, Addison-Wesley, Reading (MA), 1970.
[10] H. Scher, R. Zallen, Critical density in percolation processes, J. Chem. Phys. 53 (9) (1970) 3759–3761.
[11] D.P. Bentz, E.J. Garboczi, Percolation of phases in a three-dimensional cement paste microstructure model, Cem. Concr. Res. 21 (1991) 325–344.
[12] E.J. Garboczi, D.P. Bentz, The effect of statistical fluctuation, finite size error, and digital resolution on the phase percolation and transport properties of the NIST cement hydration model, Cem. Concr. Res. 31 (2001) 1501–1514.
[13] D.P. Bentz, E.J. Garboczi, C.J. Haecker, O.M. Jensen, Effects of cement particle size distribution on performance properties of Portland cement-based materials, Cem. Concr. Res. 29 (1999) 1663–1671.
[14] E.J. Garboczi, D.P. Bentz, Modeling of the microstructure and transport properties of concrete, Constr. Build. Mater. 10 (1996) 293–300.
[15] J. Hu, P. Stroeven, Morphological analysis and modeling of cement structure, in: M.J. Setzer, R. Auberg, H.J. Keck (Eds.), From Nano-Structure and Pore Solution to Macroscopic Behavior and Testing, Proceedings of the 2nd International Essen Workshop on Frost Resistance of Concrete, RILEM, Cachan Cedex, 2002, pp. 29–36.
[16] G. Ye, J. Hu, K. van Breugel, P. Stroeven, Characterization of the development of microstructure and porosity of cement-based materials by numerical simulation and ESEM image analysis, Mater. Struct. 35 (2002) 603–613.
[17] M. Stroeven, H. Askes, L.J. Sluys, A numerical approach to determine representative volumes for granular materials, in: H.A. Mang, F.G. Rammerstorfer, J. Eberhardsteiner (Eds.), Proceedings of the 5th World Congress on Computation Mechanics, Vienna, 2002 (proceedings published on CD).
[18] L. Holliday, Geometric consideration and phase relationships, in: L. Holliday (Ed.), Composite Materials, Elsevier, Amsterdam, 1966, pp. 1–27.
[19] J. Hu, P. Stroeven, Application of image analysis to assessing critical pore size for permeability prediction on cement paste, Image Anal. Stereol. 22 (2) (2003) 97–103.
[20] K. van Breugel, Simulation of hydration and formation of structure in hardening cement-based materials, PhD thesis, Delft University of Technology, Delft, 1991.
[21] P.G. Hoel, Introduction to Mathematical Statistics, 4th edition, Wiley, New York, 1971, pp. 226–231.
[22] P. Stroeven, Some aspects of the micromechanics of concrete, PhD thesis, Delft University of Technology, Delft, 1973.
[23] L.J. Parrott, R.G. Patel, D.C. Killoh, H.M. Jennings, Effect of age on diffusion in hydrated alite cement, J. Am. Ceram. Soc. 67 (1984) 233–237.
[24] T.C. Powers, Structure and physical properties of hardened Portland cement paste, J. Am. Ceram. Soc. 41 (1958) 1–6.
[25] J. Hu, P. Stroeven, Depercolation threshold of porosity in model cement: Approach by morphological evolution during hydration, Cem. Concr. Compos. (in press).